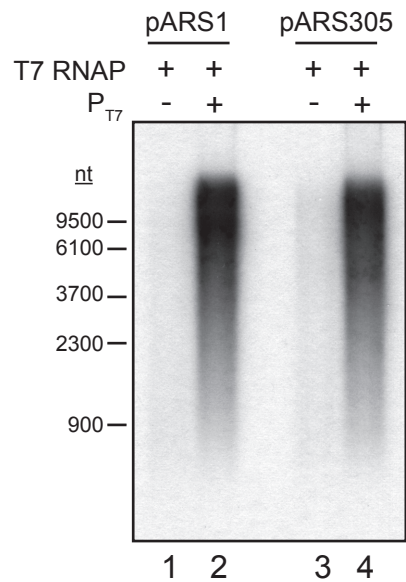
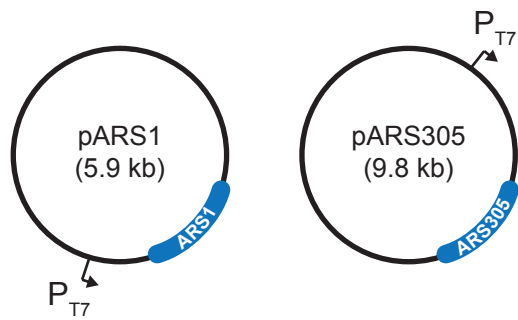


Figure S1

**A**



**B**

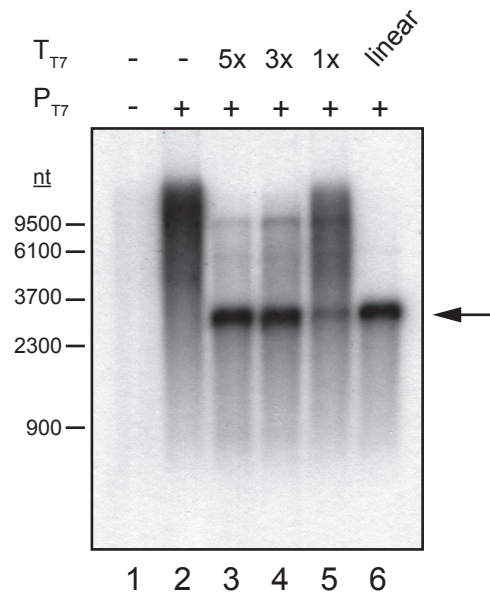
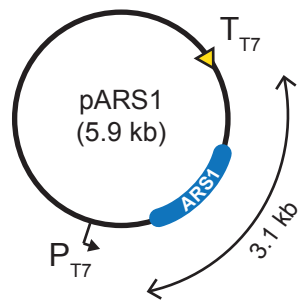
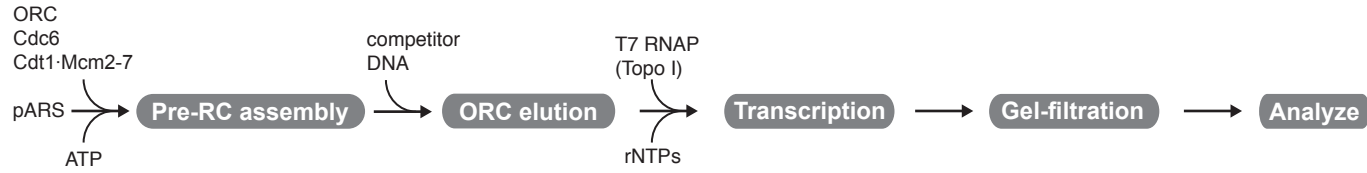
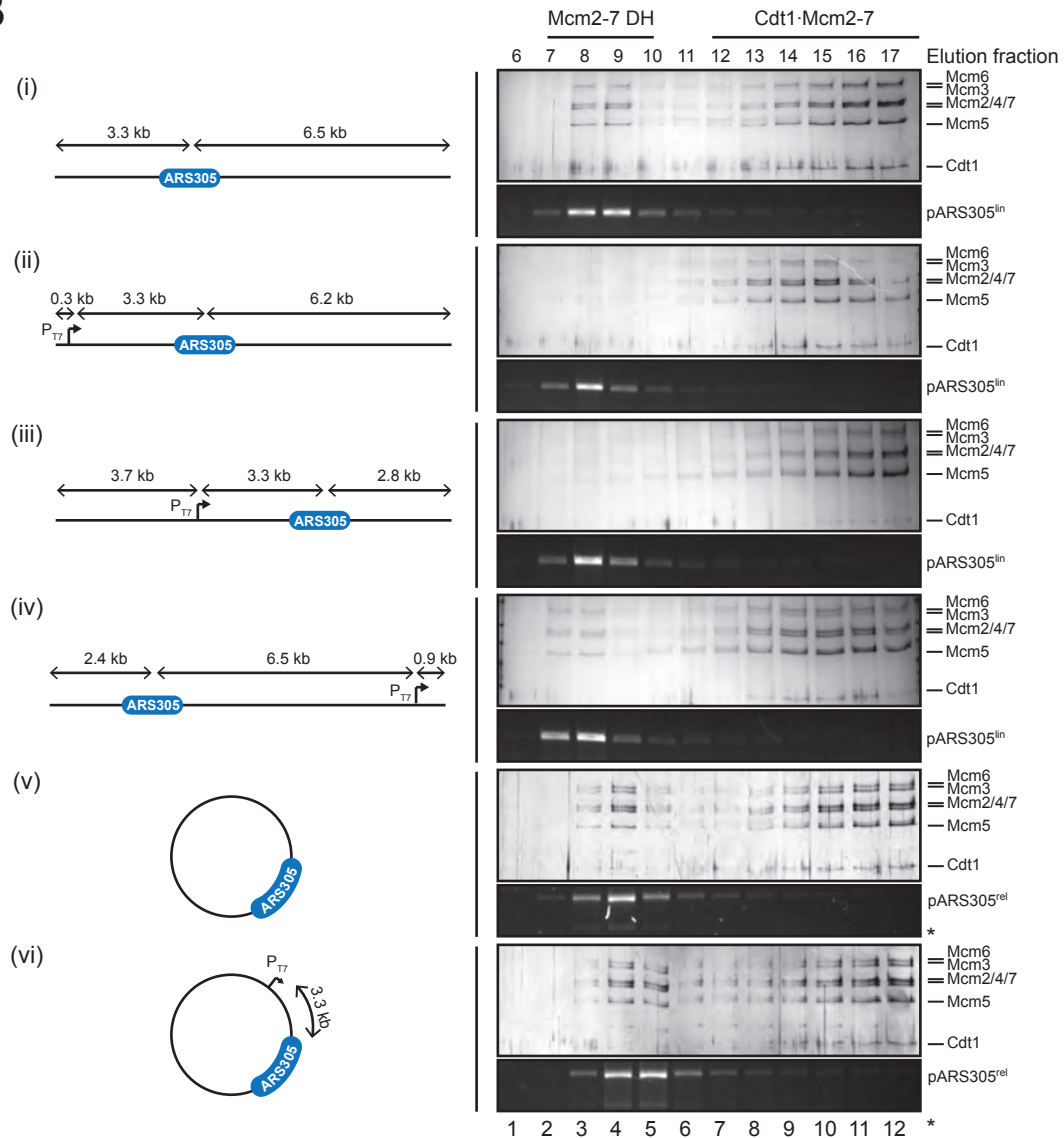


Figure S2

**A**



**B**



**C**

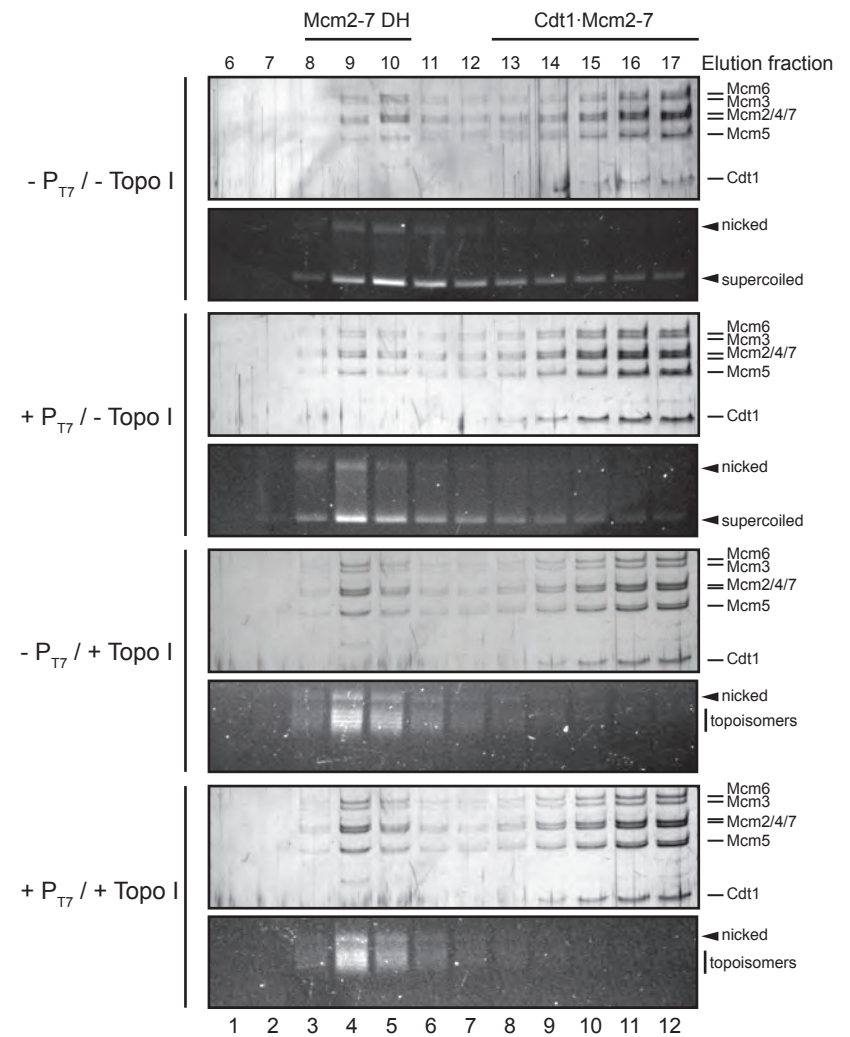


Figure S3

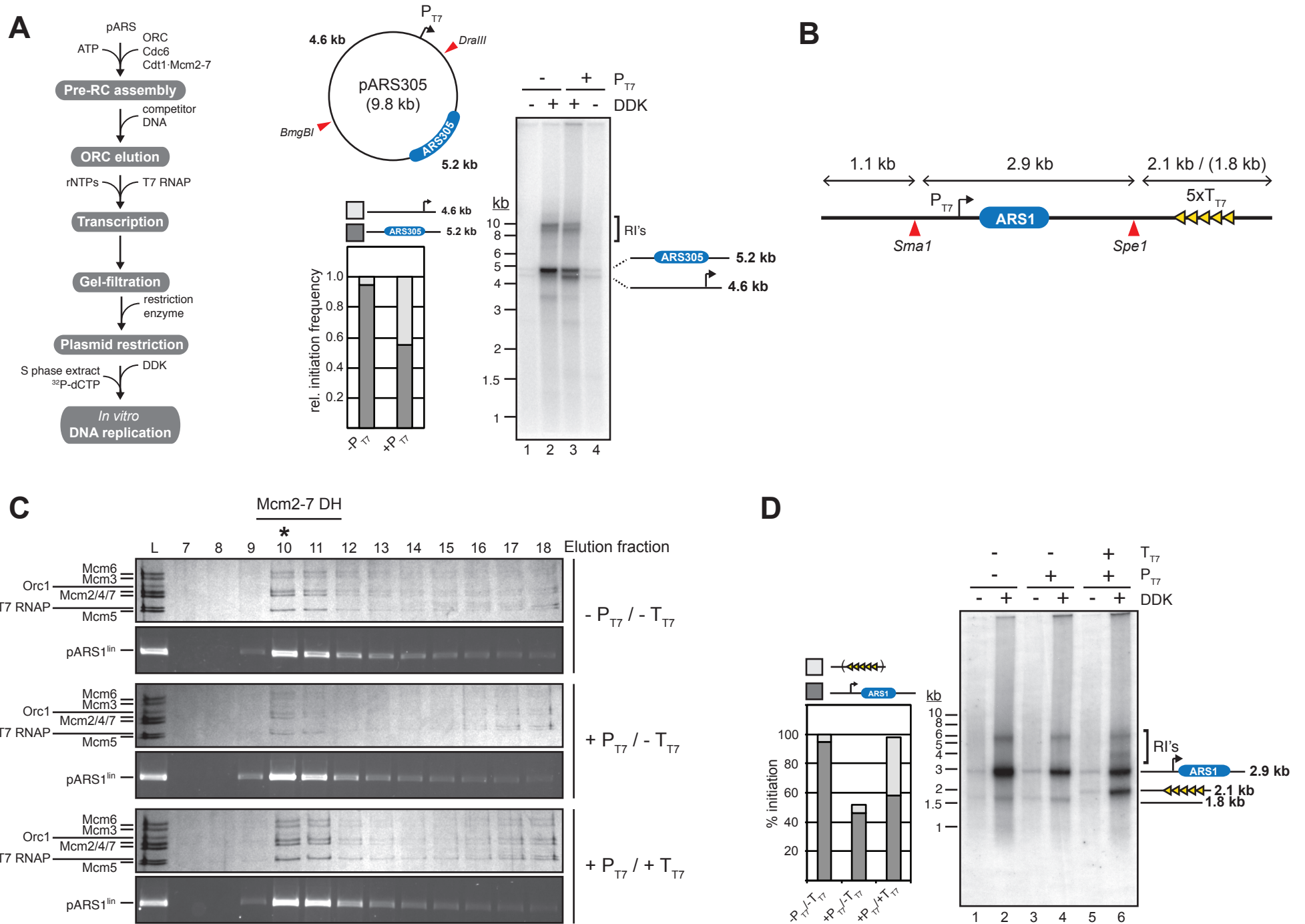


Figure S4

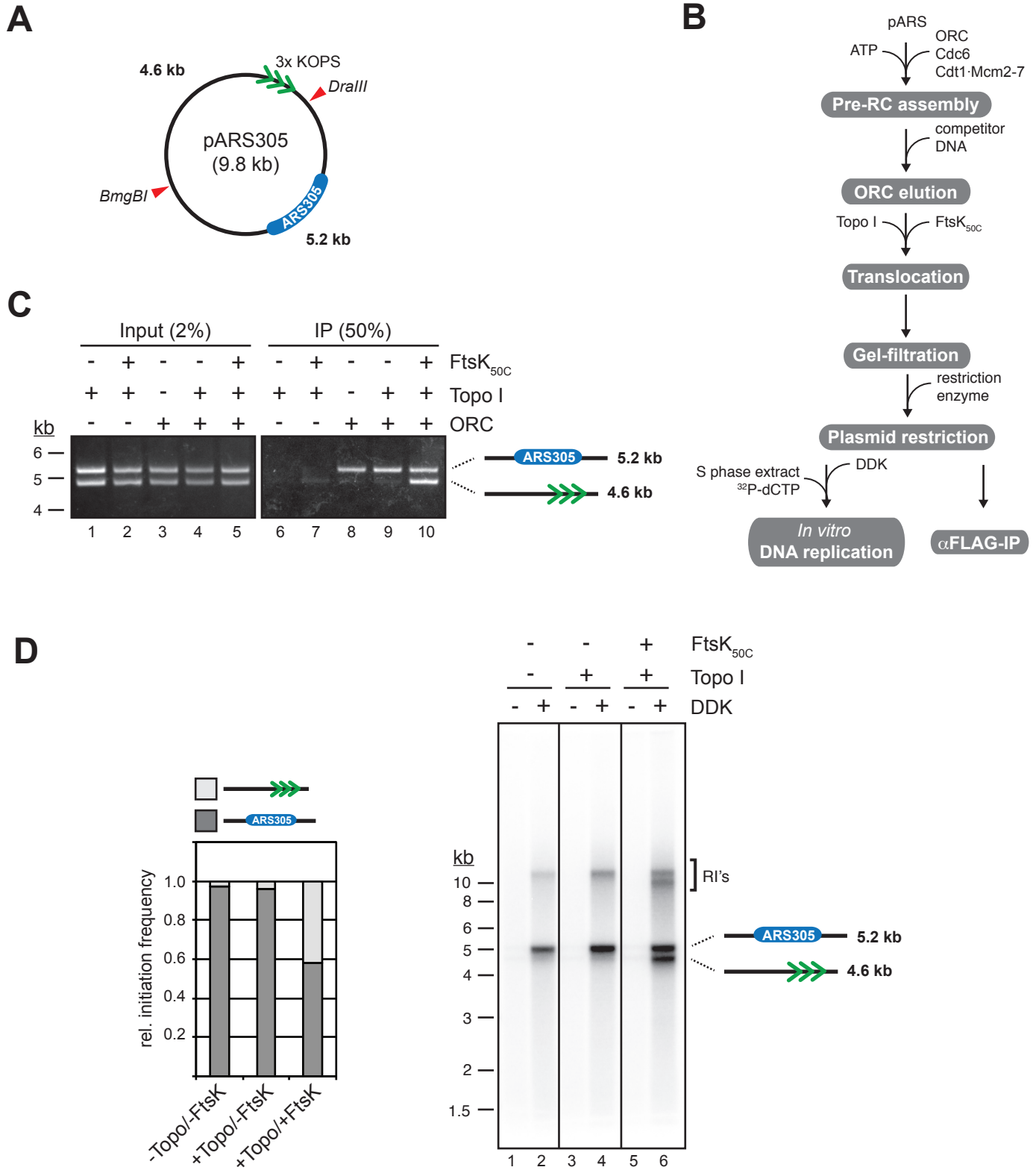
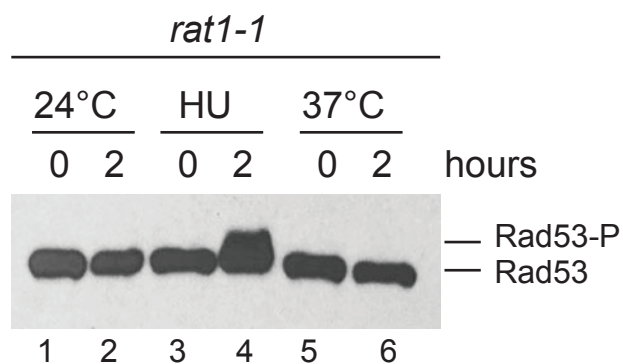
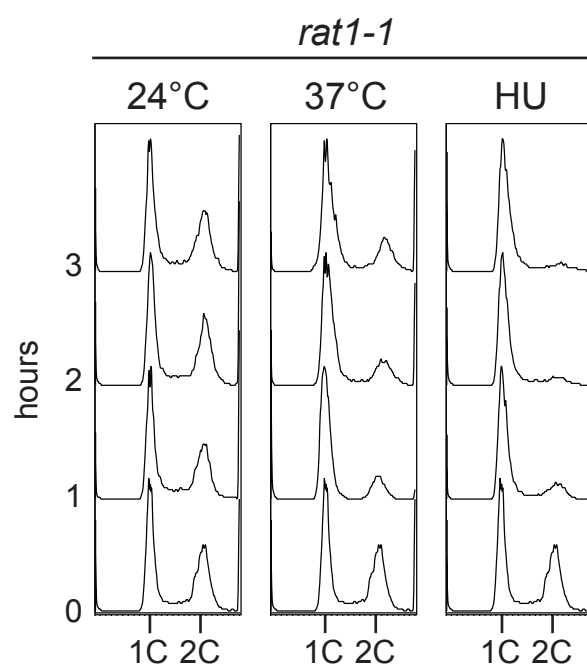


Figure S5

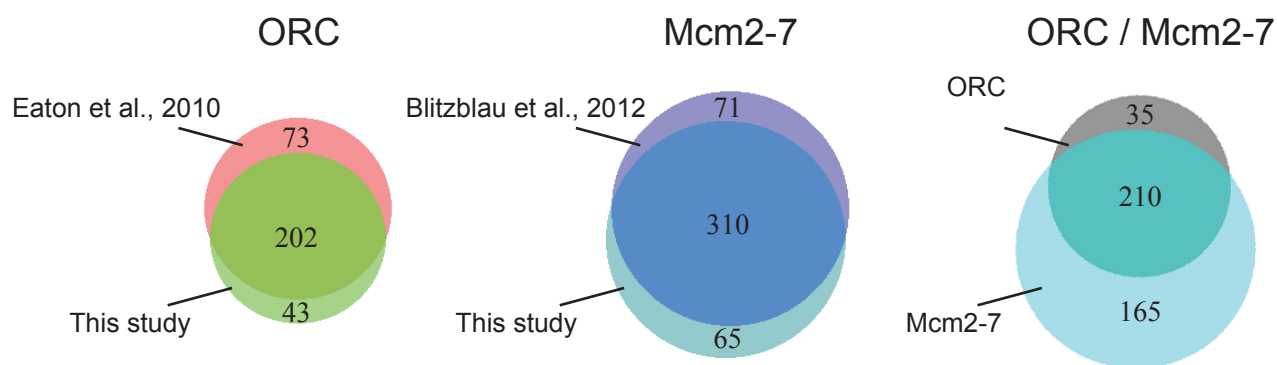
**A**



**B**



**C**



**D**

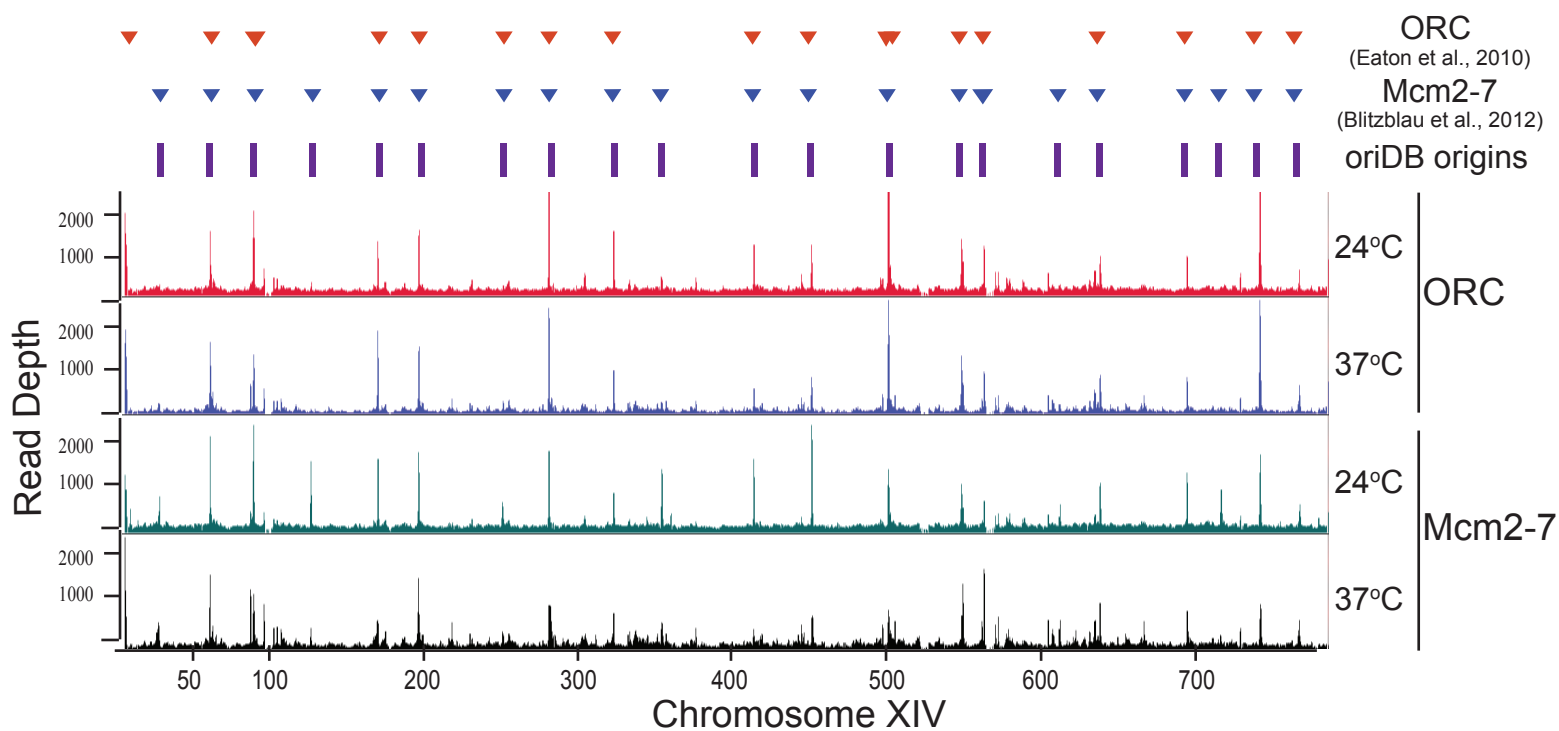


Figure S6

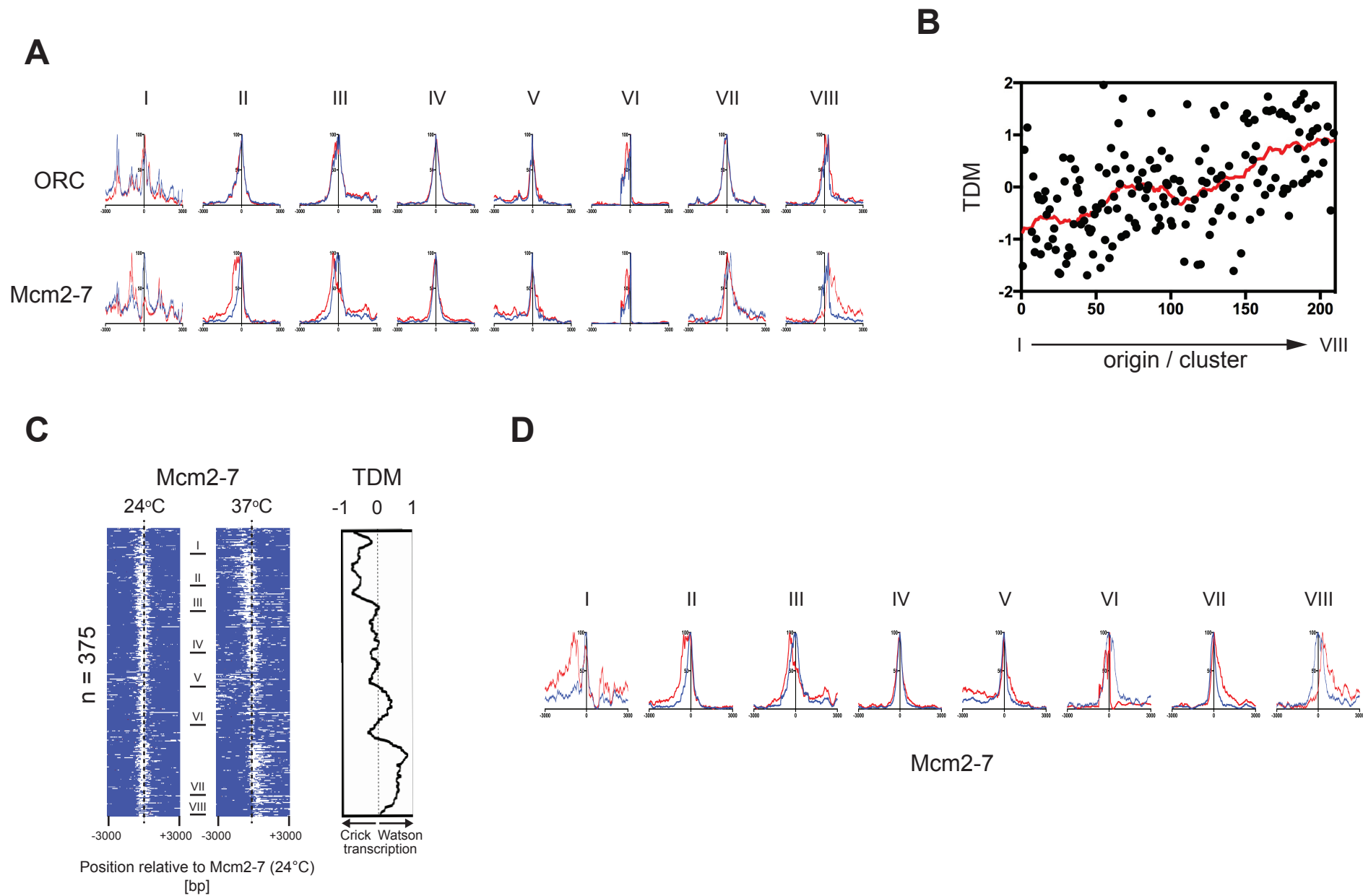
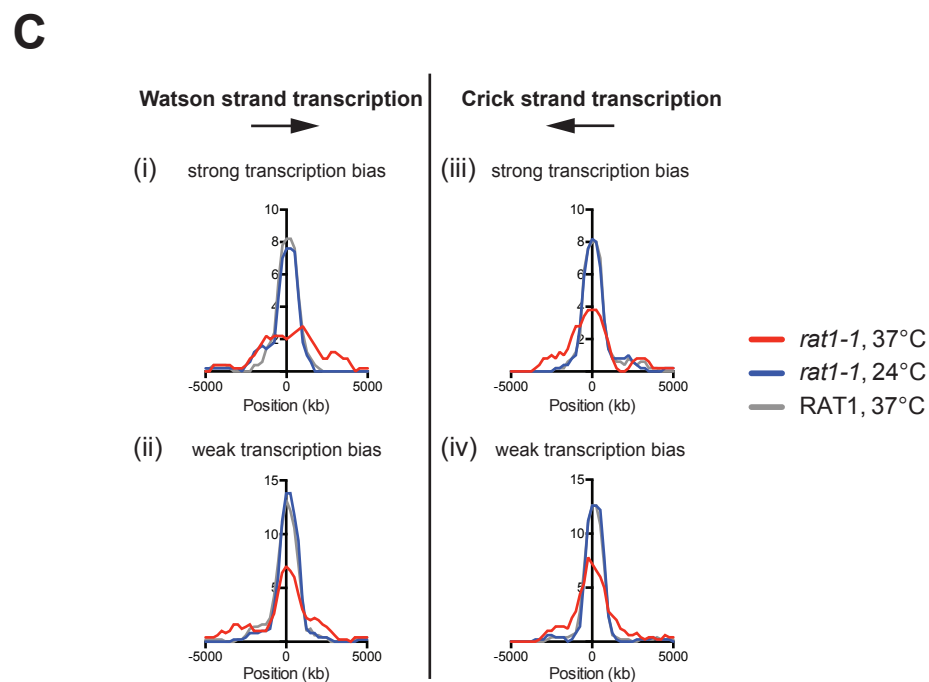
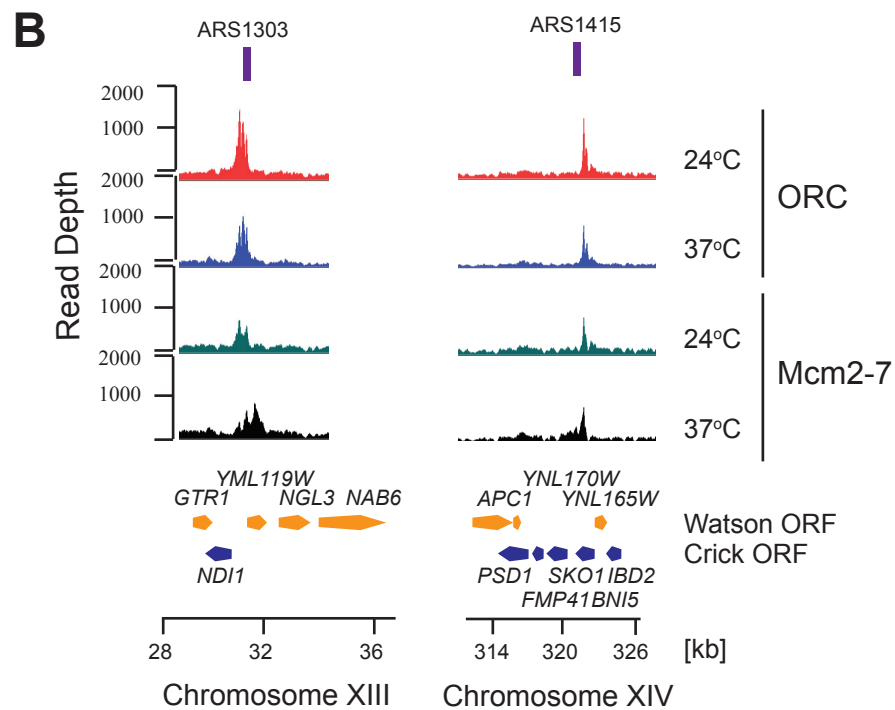
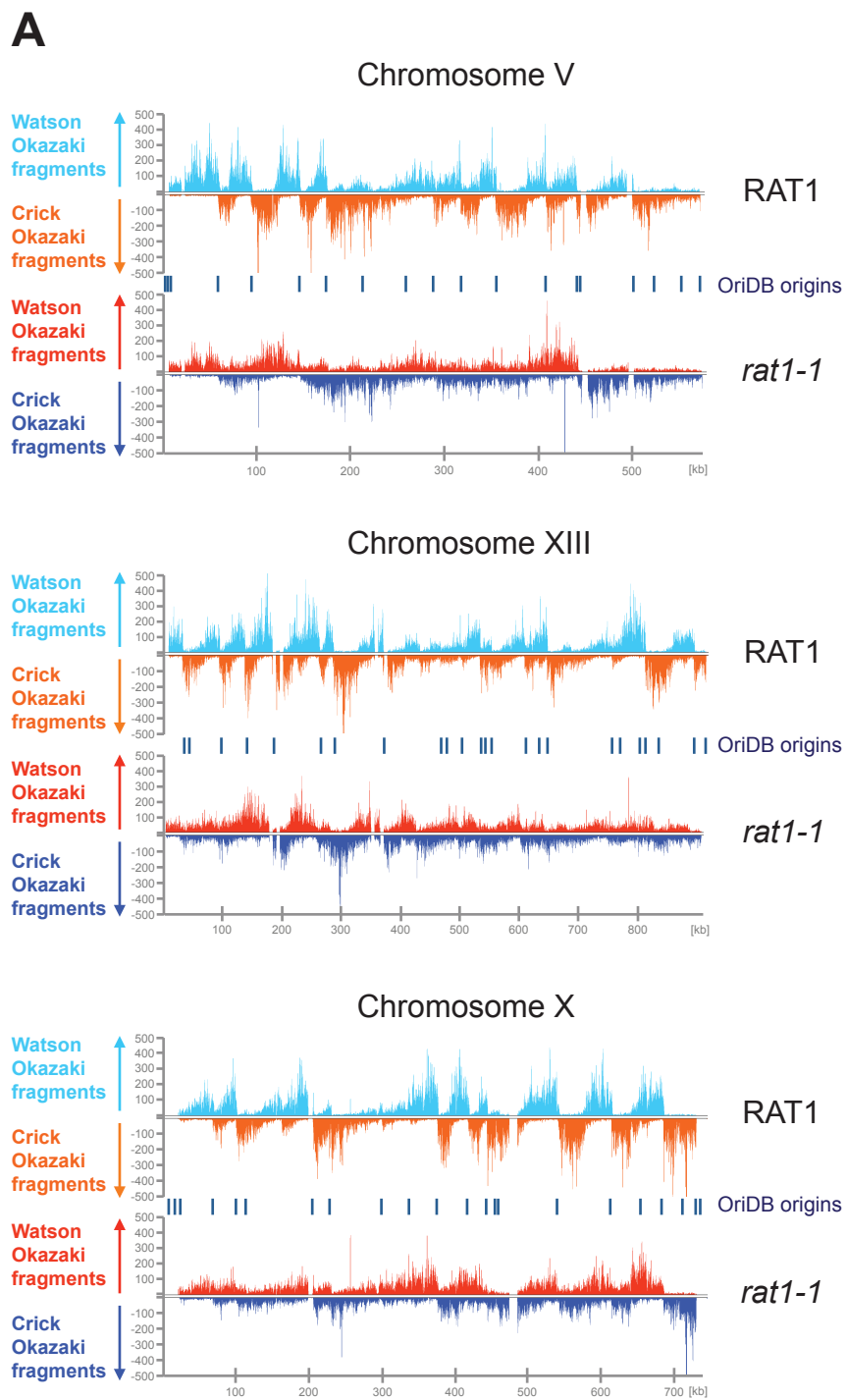


Figure S7



## Supplemental Figure Legends

### Figure S1 (related to Figures 2 and 3)

***In vitro* transcription of plasmid templates by T7 RNAP.** (A) Indicated plasmids were subjected to *in vitro* transcription in the presence of  $^{32}\text{P}$ -CTP with purified T7 RNAP in pre-RC assembly buffer. Transcripts were analyzed by formaldehyde agarose gel-electrophoresis and autoradiography. T7 promoter ( $P_{\text{T7}}$ ) was optionally included as indicated. (B) Termination efficiency of T7 transcription was tested using one, three, or 5 tandem copies of T7 terminator ( $T_{\text{T7}}$ ). pARS1 linearized at the terminator site was used as a control (lane 6). Transcripts were analyzed by formaldehyde agarose gel-electrophoresis and autoradiography.

### Figure S2 (related to Figure 2)

**T7 RNAP can push Mcm2-7 DHs off the ends of linear DNA.** (A) Reaction scheme. (B) Pre-RCs were tested for displacement by T7 RNAP on linear or circular relaxed forms of pARS305 as indicated and analyzed by gel-filtration after incubation with T7 RNAP according to reaction scheme. Proteins were analyzed by silver stain, DNA by ethidium-bromide stain. (C) Pre-RCs were reconstituted on negatively supercoiled pARS305 and analyzed by gel-filtration after transcription by T7 RNAP according to reaction scheme in a. *Vaccinia* Topo I was optionally included during the transcription step as indicated. Proteins were analyzed by silver stain, DNA by ethidium-bromide stain.

### Figure S3 (related to Figure 3)

**Mcm2-7 DHs displacement by T7 RNAP on pARS305 and linear pARS1.** (A) *In vitro* DNA replication analysis using Mcm2-7/DNA fragment complexes obtained on pARS305 as outlined in reaction scheme on left. Plasmid map and used restriction sites used are shown. Replication products were analyzed by native agarose gel-electrophoresis and  $^{32}\text{P}$  incorporation into respective fragments quantitated by phosphorimaging. (B) Map of linear derivative of pARS1 used in C and D. (C) Gel-filtration analysis of Mcm2-7 DH persistence on indicated linear pARS1 templates after incubation of pre-RCs with T7 RNAP analogous to reaction scheme in Fig. 3C; protein was analyzed by silver stain, DNA by ethidium bromide stain. The peak fraction of each reaction (#10) is marked by “ \* ”. L = load. (D) *In vitro* replication analysis after *Sma*I / *Spe*I digestion of peak fractions obtained in C. Replication products were analyzed by native agarose gel-electrophoresis and  $^{32}\text{P}$  incorporation into respective fragments quantitated by phosphorimaging.



### Figure S4 (related to Figure 3)

**Mcm2-7 DH relocation by FtsK<sub>50C</sub>.** For this analysis we used an FtsK variant, FtsK<sub>50C</sub>, which lacks an N-terminal transmembrane domain that is not required for hexamerization or ATP-dependent DNA translocation (Aussel et al., 2002). FtsK loads preferentially and in a defined orientation at 8 bp sequence motifs, termed KOPS (FtsK orienting polar sequence) (Graham et al., 2010; Lee et al., 2012; Lowe et al., 2008). We, therefore, inserted a triple KOPS cassette in pARS305 to direct FtsK<sub>50C</sub> loading. **(A)** Map of pARS305 containing three tandem copies of KOPS (green arrowheads) integrated 2.8 kb upstream of, and oriented towards, ARS305. Red triangles indicate the position of restriction sites used for the analyses in (C) and (D). **(B)** Reaction scheme. Following pre-RC assembly, ORC was eluted from the template plasmid, and FtsK<sub>50C</sub> added to the reaction alongside Topo I to avoid accumulation of potential topological strain. The reaction was subsequently gel-filtered in buffer without ATP to inhibit further translocation and promote FtsK<sub>50C</sub> release, and isolated plasmids were digested with restriction enzyme to yield a 5.2 kb ARS305-containing fragment, and a 4.6 kb vector backbone-containing fragment. **(C)** Co-immunoprecipitation of pARS305 fragments with FLAG-Mcm3. In the absence of FtsK, Mcm2-7 DHs were preferentially associated with the ARS305-containing DNA fragment; addition of FtsK<sub>50C</sub> induces a redistribution of Mcm2-7 DHs around the plasmid **(D)** *In vitro* replication analysis after Mcm2-7 DH displacement by FtsK<sub>50C</sub>. Replication products were analyzed by native agarose gel-electrophoresis and autoradiography (right panel), and <sup>32</sup>P-dCTP incorporation quantitated by phosphorimager analysis (left panel). DNA replication initiates preferentially on the ARS-containing fragment in the absence of FtsK<sub>50C</sub>, while addition of FtsK<sub>50C</sub> results in a randomization of initiation events.

### Figure S5 (related to Figures 4)

**ChIP-seq analysis of ORC and Mcm2-7 chromosomal positions in *rat1-1* cells.** **(A)** Strain YDR118 (*rat1-1* Rad53-FLAG) was grown for two hours at 24°C (lanes 1,2), or for two hours at 24°C / 200 mM hydroxyurea (HU; lanes 3,4), or for two hours at 37°C (lanes 5,6), and Rad53 phosphorylation assessed by Western blot analysis using anti-FLAG M2 antibody. HU treatment, but not shift to 37°C, induces Rad53 phosphorylation, indicative of checkpoint activation. **(B)** Nuclear DNA content of YIW138 (*rat1-1*) cells was determined by FACS analysis at indicated time points after growth at 24°C, or at 24°C / 200 mM hydroxyurea, or at 37°C. HU treatment, but not shift to 37°C, induces loss of cells with fully replicated DNA. **(C)** Venn diagrams; left: overlap between the 245 ORC peaks identified in this study and 275 ORC peaks

identified in earlier study (Eaton et al., 2010); middle: overlap between 375 Mcm2-7 peaks identified in this study and 381 Mcm2-7 peaks identified in earlier study (Blitzblau et al., 2012); right: overlap between the 245 ORC peaks and 275 Mcm2-7 peaks identified in this study. **(D)** Read depths for ChIP-seq signals across chromosome XIV in *rat1-1* cells for ORC and Mcm2-7 at 24°C or 37°C as indicated. Red inverted triangles indicate ORC peak positions identified in earlier study (Eaton et al., 2010), blue inverted triangles indicate positions of Mcm2-7 peak positions identified in earlier study (Blitzblau et al., 2012), purple bars indicate origin positions as annotated in oriDB (<http://cerevisiae.oridb.org/>).

#### **Figure S6 (related to Figure 4)**

##### **Mcm2-7, but not ORC, peak positions shift in *rat1-1* cells at non-permissive temperature.**

**(A)** Average position of ORC and Mcm2-7 within clusters I-VIII (Figure 4B). Enrichment was averaged within each cluster and plotted over a 6 kb window centered on ORC peak position at 24°C or Mm2-7 peak position at 24°C, respectively. Red: Average enrichment at 37°C; blue: average enrichment at 24°C. **(B)** TDM scores for each of the 210 origin positions (ORC/Mcm2-7 peaks). Origins are ordered according to cluster analysis for Mcm2-7 positions at 37°C. Red line: Moving average obtained across 20 nearest neighbors for each origin site. **(C)** Heat maps of Mcm2-7 enrichment at 375 Mcm2-7 peaks. Positive signal within 6 kb window is indicated in white. Mcm2-7 maps are centered on Mcm2-7 peak positions at 24°C, and Mcm2-7 peaks obtained at 37°C were ordered into eight clusters (I-VIII). Mcm2-7 (24°C) maps were subsequently ordered according to Mcm2-7 (37°C). Panel on the right indicates average TDM at respective origin sites. **(D)** Average position of Mcm2-7 within clusters I-VIII. Enrichment was averaged within each cluster and plotted over a 6 kb window centered on Mm2-7 peak position at 24°C. Red: Average enrichment at 37°C; blue: average enrichment at 24°C.

#### **Figure S7 (related to Figures 5 to 7)**

**Origin positions in *rat1-1* and RAT1 cells.** **(A)** Enrichment of Okazaki fragments mapping to the Watson and Crick strands of Chromosomes V, X, and XIII is shown for RAT1 (Light blue / orange) or *rat1-1* (red / dark blue) cells grown for 2 hours at 37°C. **(B)** ORC and Mcm2-7 enrichment around ARS1303 and ARS1415 at 24°C and 37°C is plotted over chromosomal position. Annotated ORFs on the Watson (yellow) and Crick (blue) strands are indicated. **(C)** Origin positions were determined in *rat1-1* and RAT1 control cells grown at 24°C or 37°C as indicated and plotted relative to their position in wildtype cells previously determined at 30°C (McGuffee et al., *Mol Cell*. 2013, 50:123-35). Origins were binned according to their location in

regions with strong transcription bias (TDM = 1 to 2 for Watson strand transcription; TDM = -1 to -2 for Crick strand transcription) or weak transcription bias (TDM = 0 to 1 for Watson strand transcription; TDM = 0 to -1 for Crick strand transcription).

### Supplemental Table S1: Yeast strains used in this study (related to Experimental Procedures)

Strain	Genotype
YDR95	<i>MATa ade2-1 ura3-1 his3-11,15 trp1-1 leu2-3,112 can1-100 pep4::kanMX bar::hphNAT1 (hygromycinB) cdc7-4 cir- GAL-SLD2/DPB11 (LEU2) Gal-SLD3/SLD7 (URA3) GAL-CDC45 (TRP1)</i>
YIW347	<i>MATa, his3-1, leu2-0, met15-0, ura3-0, cdc9::tetO7-CDC9-cmv_Laci-NAT</i>
YJG15	<i>MATa ade2-1 ura3-1 his3-11,15 trp1-1 leu2-3,112 can1-100 ura3-52 trp1Δ63 leu2Δ1 GAL2+ rat1-1 cdc9::tetO7-CDC9-cmv_Laci-NAT (natNT2)</i>
YDR118	<i>MATa ura3-52 trp1Δ63 leu2Δ1 GAL2+ rat1-1 RAD53::RAD53-FLAG (kanMX)</i>
YIW138	<i>MATa ura3-52 trp1Δ63 leu2Δ1 GAL2+ rat1-1</i>

### Supplemental Experimental Procedures

#### DNA templates

A T7 promoter was inserted between EcoRV and NcoI sites into pARS/WTA (Marahrens and Stillman, 1992) to generate p828. T7 terminator ( $T_{T7}$ ) sequences were derived from pET expression vector and inserted via BmgBI / Bsu36I into p828 to yield p829 (single copy of  $T_{T7}$ ), or p850 (five tandem copies of  $T_{T7}$ ). To generate p620, a T7 promoter was inserted at the BglII site of pARS305 (Gros et al., 2014). A triple KOPS element (Graham et al., 2010) was inserted via BglII into pARS305 (Gros et al., 2014) to generate p580.

#### Proteins

ORC, Cdt1•MCM2-7, and DDK were purified as previously described (Frigola et al., 2013; Gros et al., 2014). *S. cerevisiae* Cdc6 was expressed as a GST-fusion protein in BL21 DE3 Codon+ RIL. FtsK<sub>50C</sub> was a gift of K. Mariani, Memorial Sloan-Kettering Cancer Center. *Vaccinia* virus Topo I was a gift of S. Shuman, Memorial Sloan-Kettering Cancer Center.

### ***In vitro* T7 transcription**

35 units of T7 RNA Polymerase (NEB) were mixed on ice with 0.25 pmol of plasmid in pre-RC assembly buffer supplemented with 500  $\mu$ M of each ATP / UTP / GTP / CTP, 10 mM DTT, 10 U of SUPERase·In (Life Technologies), 33 nM of [ $\alpha$ - $^{32}$ P]-ATP, and incubated for 30 minutes at 20°C. The reaction was stopped with 0.2% SDS and digested with 1.6U of Proteinase K (NEB) for 30 minutes at 37°C. The reaction was mixed with one volume of formamide / MOPS 1X buffer, heated at 65°C for 10 minutes and fractionated on a 1 % agarose gel containing 6 % formaldehyde (w/v) / MOPS 1x . The gel was dried and exposed to film or phosphor-imager.

### **Isolation of Mcm2-7 DHs after translocation by FtsK<sub>50C</sub>**

Following pre-RC assembly, the reaction was supplemented with 10 mM DTT / 5 mM ATP / 5 pmol of *Vaccinia* virus Topo I / 33.5 pmol of FtsK<sub>50C</sub>. Incubation was carried out for 30 minutes at 30°C, after which the reaction was fractionated on a 2 mL S1000 column equilibrated in buffer K / 2 mM  $\beta$ -Mercaptoethanol.

### **Supplemental References**

- Aussel, L., Barre, F.X., Aroyo, M., Stasiak, A., Stasiak, A.Z., and Sherratt, D. (2002). FtsK Is a DNA motor protein that activates chromosome dimer resolution by switching the catalytic state of the XerC and XerD recombinases. *Cell* *108*, 195-205.
- Frigola, J., Remus, D., Mehanna, A., and Diffley, J.F. (2013). ATPase-dependent quality control of DNA replication origin licensing. *Nature* *495*, 339-343.
- Graham, J.E., Sherratt, D.J., and Szczelkun, M.D. (2010). Sequence-specific assembly of FtsK hexamers establishes directional translocation on DNA. *Proceedings of the National Academy of Sciences of the United States of America* *107*, 20263-20268.
- Lee, J.Y., Finkelstein, I.J., Crozat, E., Sherratt, D.J., and Greene, E.C. (2012). Single-molecule imaging of DNA curtains reveals mechanisms of KOPS sequence targeting by the DNA translocase FtsK. *Proceedings of the National Academy of Sciences of the United States of America* *109*, 6531-6536.
- Lowe, J., Ellonen, A., Allen, M.D., Atkinson, C., Sherratt, D.J., and Grainge, I. (2008). Molecular mechanism of sequence-directed DNA loading and translocation by FtsK. *Molecular cell* *31*, 498-509.
- Marahrens, Y., and Stillman, B. (1992). A yeast chromosomal origin of DNA replication defined by multiple functional elements. *Science* *255*, 817-823.